Diagnosability Index and Its Application to Bearing Fault Diagnosis

Ankush C. Jahagirdar and K. K. Gupta

Abstract Bearings are essential component of rotating machines and are often prone to failure. Early detection of bearing faults thus becomes important for predictive maintenance strategies. Conventionally, vibration measurement is considered to be the most reliable and widely used indicator of fault signatures, which are to be extracted from the raw signal. Traditional signal processing techniques, like envelope spectrum, are employed for extraction of such features. However, selection of optimal band and center frequency remains the main objective of research in the field. Use of spectral kurtosis (kurtogram) is now a standard method for this selection. However, a benchmark study on Case Western Reserve University dataset shows several non-diagnosable cases using kurtogram method. The purpose of this study is to quantify diagnosability in the form of an index and use it as a selection criterion for getting optimal band and center frequency. The proposed method is validated using non-diagnosable cases of the benchmark study, and the results are compared with that of conventional Hilbert transform method and autogram method.

Keywords Fault diagnosis · Diagnosability index · Vibration monitoring

Nomenclature

BPFI	Ball pass frequency inner race
BPFO	Ball pass frequency outer race
BSF	Ball spin frequency
HT	Hilbert transform
SES	Squared envelope spectrum
DI	Diagnosability index

A. C. Jahagirdar (✉) · K. K. Gupta
Birla Institute of Technology & Science, Pilani, Rajasthan 333031, India
e-mail: ankush.chandrakant@pilani.bits-pilani.ac.in

K. K. Gupta
e-mail: kgupta@pilani.bits-pilani.ac.in

J. S. Rao et al. (eds.), *Proceedings of the 6th National Symposium on Rotor Dynamics*, Lecture Notes in Mechanical Engineering,
https://doi.org/10.1007/978-981-15-5701-9_29

1 Introduction

Vibration signals are most reliable way of monitoring faults in rotating machinery. When a fault occurs on either the inner raceway, outer raceway, or on the rolling element of a bearing, it can be captured using accelerometer sensor located in contact with the machine. The high-frequency shock signal generated due to impact of fault is very peculiar and often shows amplitude modulation. The cyclostationary nature of such signals is well known and of specific interest from signal processing point of view. Complex nature of these signals and random interfering noise makes it difficult to model such signals. It is often very difficult to find the optimum resonance band for filtering out undesired components from the signal. State-of-the-art research focuses mainly on this aspect of finding the optimum center frequency and bandwidth, and the various statistical features are used to guide this optimization process. Kurtosis is one such feature which is very widely used. A study on Case Western Reserve University dataset uses spectral kurtosis as a benchmark and classifies the cases into easily diagnosable, partially diagnosable and non-diagnosable [1, 2]. This benchmark method mainly relies on kurtosis as an indicator of fault in time domain signal and thus finds optimal band and center frequency by finding the maximum value of kurtosis. However, there are several cases in which this method fails, and thus, this method of kurtogram was further modified into infogram [3], sparsogram [4, 5], and autogram [6].

Different signal processing methods are proposed to extract bearing fault features such that the size and type of fault is faithfully represented. A detailed analysis of different cepstral editing methods is discussed in [7]. On the other hand, signal processing methods based on probability distribution function of the fault signal are also being explored [8]. Cepstral analysis is used a way of filtering different than traditional Fourier spectrum based methods [9–13]. A brief history of few such methods is discussed by Randall in [14]. Out of these, automated cepstral editing procedure [15] and cepstral prewhitening [11] are important signal preprocessing methods which try to improve the diagnosability by removing stationary harmonic component from the signal.

Unlike these methods, the proposed method focuses on features local to each potential fault frequency. Though, in the benchmark study, the classification of cases is based on classical fault signatures like fault frequency and harmonics, sidebands, etc., it is not possible to quantify all of these. Thus, we define diagnosability in terms of simple quantifiable parameters like amplitude at fault frequency, deviation of fault frequency from the theoretical value, and number of significant peaks in the spectrum. The diagnosability index, thus designed, is used as a feature to select optimum band and center frequency. Cases in which the proposed method performs better than the benchmark method are discussed.

2 Diagnosability

A close observation of the CWRU dataset reveals that the fault diagnosis largely depends on following factors:

1. Amplitude at fault frequency and its harmonics,
2. Deviation of peak frequency from theoretical fault frequency,
3. Number of other significant peaks in the spectrum,
4. Sidebands in case of inner race and ball fault signals.

Based on this observation, the diagnosability index is proposed as:

$$\mathrm{DI} = \mathrm{A.D.P} \tag{1}$$

where, A is the amplitude at the fault frequency, D is derived from the deviation of fault frequency from its theoretical value, and P is derived from the number of other significant peaks in the spectrum.

The block diagram of the proposed method is shown in Fig. 1. As the fault signal is modulated, the conventional method of band-pass filtering and demodulating is used to find the squared envelope spectrum (SES) of the vibration signal. Full-tree wavelet packet transform (WPT), with db1 as mother wavelet, is applied to decompose the signal without reducing the length of the signal. The decomposed signal is then Hilbert transformed to find its envelope. To find out this values of A, D and P, the value of fault frequency has to be known. As the fault frequencies of inner race fault, outer race fault and rolling element fault are different, three different values of diagnosability index DI_I, DI_O and DI_R are calculated respectively.

The values of fault frequencies are theoretically calculated based on the geometry of the bearing using following formulae [16].

$$f_{\mathrm{or}} = f_{\mathrm{s}} \frac{N_{\mathrm{b}}}{2} \left(1 - \frac{B_{\mathrm{d}}}{P_{\mathrm{d}}} \cos \emptyset\right) \tag{2}$$

$$f_{\mathrm{ir}} = f_{\mathrm{s}} \frac{N_{\mathrm{b}}}{2} \left(1 + \frac{B_{\mathrm{d}}}{P_{\mathrm{d}}} \cos \emptyset\right) \tag{3}$$

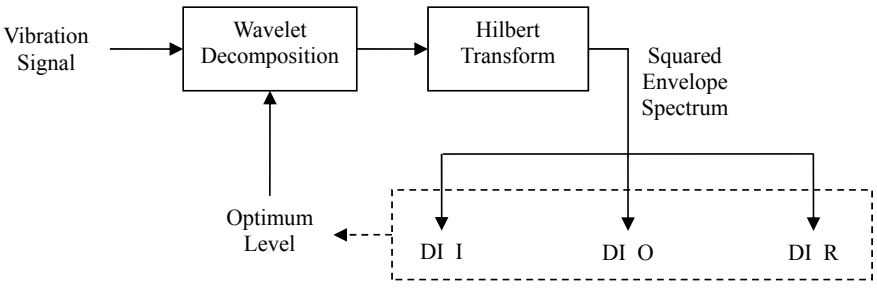

Fig. 1 Block diagram of the proposed method

$$f_{\mathrm{re}} = f_{\mathrm{s}} \frac{P_{\mathrm{d}}}{2B_{\mathrm{d}}} \left(1 - \frac{B_{\mathrm{d}}^2}{P_{\mathrm{d}}^2} (\cos \emptyset)^2\right) \tag{4}$$

where f_{s} is the rotational speed in Hz, N_{b} is the number of rolling elements, B_{d} is the diameter of rolling elements, P_{d} is the pitch diameter, $\emptyset$ is the contact angle, and f_{or}, f_{ir}, f_{re} are the fault frequencies of outer race fault, inner race fault, and rolling element fault (BPFI, BPFO, and BSF), respectively.

*2.1 Amplitude (***A***)*

To ensure that the diagnosability index (DI) has a value in the interval [0,1], each feature is scaled in this interval by simple linear transformation. The amplitudes of spectral peaks are scaled by dividing each value by the maximum value. This feature tells how significant the peak at the fault frequency is and it directly affects diagnosis, in a sense, that if there is a large peak at the fault frequency, then it signifies presence of fault.

Though the theoretical value of the fault frequency is known, it is often observed that the actual value of fault frequency is slightly different. This is because of two main reasons—first, the uncertainty and error associated with the speed sensor and second, the cyclostationary nature of the signal. As mentioned by Randall et al. [16], this deviation is generally 1–2%. Considering this, we have introduced a tolerance of ± 2 Hz, and taken the maximum peak in the frequency interval of $[f - 2, f + 2]$.

*2.2 Deviation (***D***)*

As the fault frequency is bound to have some uncertainty in its value, it is very difficult, especially cases where the fault signal is submerged in noise, to pinpoint this frequency in the spectrum. With the introduction of tolerance band, there is a possibility of choosing a wrong value of frequency. To avoid this, the proposed index linearly penalizes the deviation of frequency from its theoretical value assuming that large deviation from the theoretical value means that it is unlikely to be the fault frequency. This difference in theoretical and actual frequencies is also scaled to [0,1] interval.

$$D = \frac{2 - |(\text{Actual} - \text{Theoretical})|}{2} \tag{5}$$

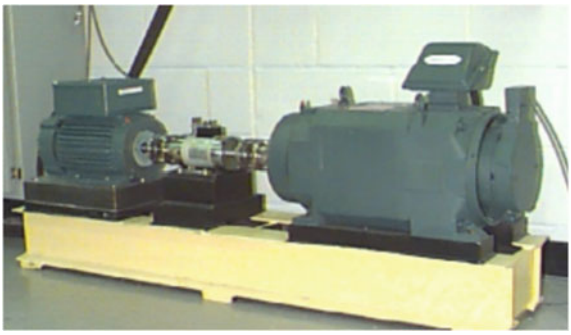

Fig. 2 Case Western Reserve University experimental set-up

*2.3 Peaks (***P***)*

It is quite clear that the amplitude of fault peak alone is not sufficient to quantify diagnosability. It has to be observed in relation to other significant peaks in the spectrum. If the number of significant peaks other than the fault harmonics is more, then that case is either partially or not diagnosable. Thus, the third feature to calculate DI is selected to be number of other significant peaks in the spectrum. This feature has inverse relation with diagnosability and is thus calculated similar to Eq. (2), that is, number of significant peaks is subtracted from a tolerance value and then divided by the same value to scale it down to [0,1].

It should be noted that, significance is a relative term and for the purposes of this study, it is assumed to be 20% of the maximum spectral amplitude.

3 Bearing Fault Data

To substantiate the importance of the proposed method, we have used a standard dataset on bearing faults provided online by Case Western Reserve University [17]. The dataset contains vibration signals from a 2 hp electric motor setup as shown in Fig. 2 with 6205-2RS JEM SKF deep groove ball bearing at the drive end and 6203-2RS JEM SKF deep groove ball bearing at the fan end.

4 Results

The diagnosability index (DI) is first verified using a benchmark study on CWRU dataset [1]. In this study, each signal is classified into easily diagnosable, partially diagnosable, and non-diagnosable case. Figure 3 shows DI values for easily diagnosable and non-diagnosable cases of inner race, outer race, and rolling element faults. It can be observed from the figure that, barring few cases, the diagnosable

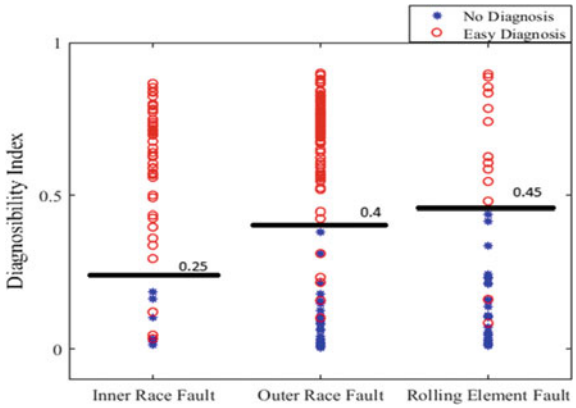

Fig. 3 Diagnosis based on diagnosability index

and non-diagnosable cases are fairly separable from each other based on the diagnosability index. Also, the value of proposed diagnosability index (DI) is larger for easy diagnosis as compared to non-diagnosable cases.

Figure 4 shows the performance of conventional Hilbert transform, the proposed method and the autogram method for three non-diagnosable cases of the benchmark study.

Case 1 is a case of drive end bearing with an outer race fault located opposite to the load zone with fault size of 7 mil, under 1 hp load. The accelerometer is located at the baseline of the setup, and it captures the raw vibration of the setup sampled at 12,000 Hz. This case is classified as a non-diagnosable case by the benchmark study because even after the decomposition, the envelope spectrum shows no classical spectrum features, like the peaks at the fault frequency and its harmonics. The location of the fault frequency and its harmonics are shown by arrows in Fig. 4. The autogram method also fails, as seen in Fig. 4c. This means that the optimum level (7) and corresponding optimum node (111) selected by the autogram method fails to enhance the fault features. The proposed method, however, chooses level 3 and node 4 of wavelet decomposition, and significant fault peaks can be observed in the envelope spectrum of the decomposed signal in Fig. 4b.

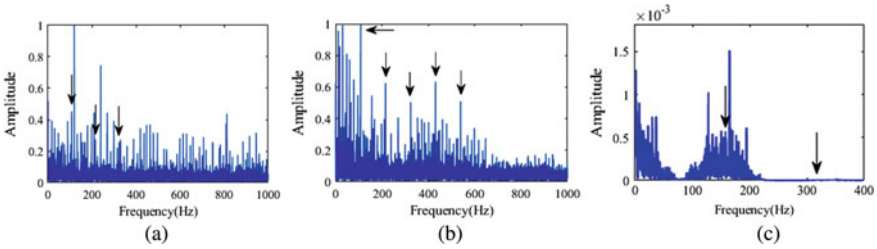

Fig. 4 Envelope spectrums for Case 1 using **a** conventional Hilbert transform, **b** proposed method, **c** autogram method

Case 2 is a case of drive end bearing with a rolling element fault of 7 mil, under 2 hp load. The accelerometer is located at the baseline of the setup, and it captures the raw vibration of the setup sampled at 12,000 Hz. The cases of rolling element faults are difficult to diagnose, because the rolling element fault behaves very similar to Gaussian noise in terms of its distribution. The distribution in such cases does not show peakedness and thus kurtosis-based methods, like kurtogram and autogram, seem to fail. From Fig. 5b, it can be observed that the proposed method identifies the optimal band as (7, 44), and the envelope spectrum of the decomposed signal shows significant fault features compared to the Hilbert transform and the autogram methods.

Case 3 is a 14 mil outer raceway fault at drive end bearing, in the load zone, and the data is collected at the baseline accelerometer. The autogram method chooses the optimum level-node pair as (7, 126) which clearly removes the fault harmonics from the spectrum as shown in Fig. 6c. The optimum node chosen by the proposed method is (7, 54). At this node, we can observe maximum peak at 1X fault frequency and small peaks at second and third harmonics as shown in Fig. 6b. This result is evidently better compared to the conventional Hilbert transform, as the fault peaks are not submerged in other peaks as shown in Fig. 6a.

As the selection of optimum node depends on maximum value of the diagnosability index, the resultant spectrum should have more peak amplitude and less number of other peaks. This can be observed in all the three representative cases.

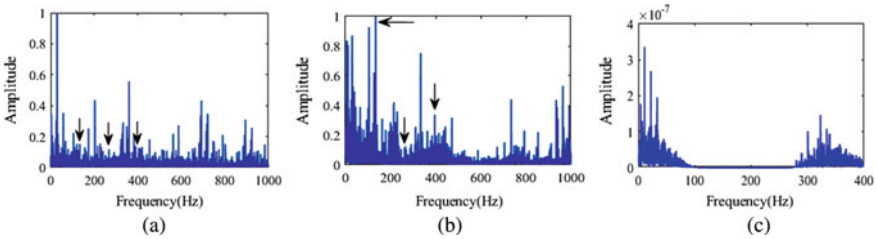

Fig. 5 Envelope spectrums for Case 2 using **a** conventional Hilbert transform, **b** proposed method, **c** autogram method

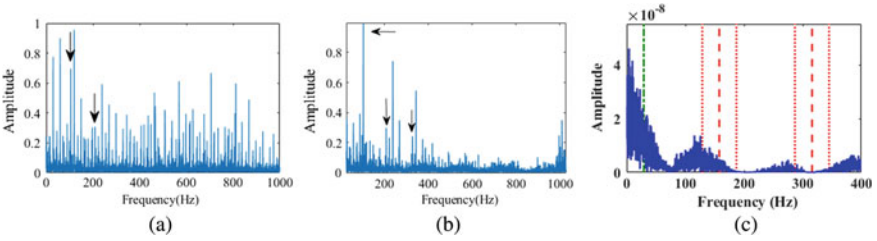

Fig. 6 Envelope spectrums for Case 3 using **a** conventional Hilbert transform, **b** proposed method, **c** autogram method

Comparison of conventional Hilbert transform spectrum and proposed method spectrum reveals that the fault peaks become more prominent compared to other peaks in the spectrum.

5 Conclusions

Current research in bearing fault diagnosis focuses mainly on the objective of finding optimum band and center frequency so that the raw vibration signal can be decomposed to show prominent fault features in the envelope spectrum. The benchmark, kurtogram method, and its modification, the autogram method, use kurtosis to guide the selection of this optimum band. However, in various non-diagnosable cases, these methods fail. To overcome this problem, the proposed method looks at local spectrum features like the fault peak amplitude, its deviation from the theoretically calculated fault frequency, and number of other significant peaks in the spectrum. A diagnosability index is designed using these parameters such that its value is larger for easily diagnosable cases than for the non-diagnosable cases. This index is used to guide the selection of optimum band. With the help of three non-diagnosable cases, the improvement in fault features is demonstrated using the proposed method over the autogram method. The diagnosability index can be improved, in future, to provide improved classification between the easily diagnosable and non-diagnosable cases and also to incorporate the partially diagnosable cases.

References

1. Smith WA, Randall RB (2015) Rolling element bearing diagnostics using the Case Western Reserve University data: a benchmark study. Mech Syst Signal Process 64–65:100–131
2. Antoni J, Randall RB (2006) The spectral kurtosis: application to the vibratory surveillance and diagnostics of rotating machines. Mech Syst Signal Process 20(2):308–331
3. Antoni J (2016) The infogram: entropic evidence of the signature of repetitive transients. Mech Syst Signal Process 74:73–94
4. Tse PW, Wang D (2013) The design of a new sparsogram for fast bearing fault diagnosis: Part 1 of the two related manuscripts that have a joint title as "Two automatic vibration-based fault diagnostic methods using the novel sparsity measurement—Parts 1 and 2". Mech Syst Signal Process 40(2):499–519
5. Tse PW, Wang D (2013) The automatic selection of an optimal wavelet filter and its enhancement by the new sparsogram for bearing fault detection: Part 2 of the two related manuscripts that have a joint title as "Two automatic vibration-based fault diagnostic methods using the novel sparsity measurement—Parts 1 and 2". Mech Syst Signal Process 40(2):520–544
6. Moshrefzadeh A, Fasana A (2018) The autogram: an effective approach for selecting the optimal demodulation band in rolling element bearings diagnosis. Mech Syst Signal Process 105:294–318
7. Peeters C, Guillaume P, Helsen J (2017) A comparison of cepstral editing methods as signal preprocessing techniques for vibration-based bearing fault detection. Mech Syst Signal Process 91:354–381

8. Mohanty S, Gupta KK, Raju KS (2017) Effect of unitary sample shifted Laplacian and rectangular distributions in bearing fault identifications of induction motor. IET Sci Meas Technol 11(4):516–524
9. Morsy ME, Achtenova G (2015) Rolling bearing fault diagnosis techniques—autocorrelation and cepstrum analyses. In: 23rd Mediterranean conference on control and automation, MED, pp 328–334
10. Salah M, Bacha K, Chaari A (2014) Cepstral analysis of the stator current for monitoring mechanical unbalance in squirrel cage motors. In: 1st International Conference on Green Energy, ICGE, pp 290–295
11. Borghesani P, Pennacchi P, Randall RB, Sawalhi N, Ricci R (2013) Application of cepstrum pre-whitening for the diagnosis of bearing faults under variable speed conditions. Mech Syst Signal Process 36(2):370–384
12. Hwang YR, Jen KK, Shen YT (2009) Application of cepstrum and neural network to bearing fault detection. J Mech Sci Technol 23(10):2730–2737
13. Li H, Ai S (2008) Application of order bi-cepstrum to gearbox fault detection. In: Proceedings of World Congress on intelligent control and automation, vol 2, No. 1, pp 1781–1785
14. Randall RB (2017) A history of cepstrum analysis and its application to mechanical problems. Mech Syst Signal Process 97:3–19
15. Ompusunggu AP (2015) Automated cepstral editing procedure (ACEP) as a signal preprocessing in vibration-based bearing fault diagnostics. In: International conference of surveillance, pp 1–11
16. Randall RB, Antony J (2011) Rolling element bearing diagnostics—a tutorial. Mech Syst Signal Process 25(2):485–520
17. Loparo KA. Bearings vibration data set. Case Western Reserve University. Available: http://csegroups.case.edu/bearingdatacenter/pages/12k-drive-end-bearing-fault-data